3D Optimisation of Average Torque of Electrostatic Micromotors

Prof. Dr. Ir R. Belmans	KU Leuven, Dep. EE, group ELEN,B-3001 Leuven, Belgium
Dr. K. Hameyer	KU Leuven, Dep. EE, group ELEN,B-3001 Leuven, Belgium
Ir. TB. Johansson	KU Leuven, Dep. EE, group ELEN,B-3001 Leuven, Belgium
Ir. M. Van Dessel	KU Leuven, Dep. EE, group ELEN,B-3001 Leuven, Belgium

Abstract

This paper presents a technique to optimise electrostatic micromotors. The finite element technique is combined with different types of optimisation strategies, of which one of them, a version of the evolution strategy will be discussed. It futher involves an automated generation of 3d meshes where the dimesions and rotor positions of the motor models can be chosen arbitrarily. It also involves constructing equivalent circuit models for the electrostatic motors. Both, the automated 3d mesh generation and the construction of the equivalent circuit model are taken into accounted in this paper. The possibility of making powerful tools in the field of optimisation will be described but also some warnings concerning the results from automated optimisation will be mentioned.

1. Introduction

The main challenge for electrostatic micromotors among other electrostatic micro mechanical devices, is still achieving enough torque to overcome the friction forces due to the small dimensions [3]. This is why optimisation of each micromotor design is a necessity to ensure or even enable good operation.

Electrostatic motors, sometimes called variable capacitance motors, consist of a specified number of stator and rotor electrodes (poles). Depending on the arangement of stator and rotor poles the electric flux of these motors can be directed perpendicular to or along the motor axis, being a radial flux or an axial flux motor respectively. Both types are investigated in.
Two numerical methods are combined to receive a self running optimisation procedure. Figure 1 illustrates the simple link between the numerical field computation and the numerical optimisation method. With a valid set of initial parameters and some additional constraints the optimisation problem is set up.

The generation of a three dimensional finite element mesh constitutes the first step. Then the set of differential field equations is solved, the equivalent circuit parameters generated and the circuit analysed for the average produced torque and/or torque-ripple. This is the evaluation of the objective function. The

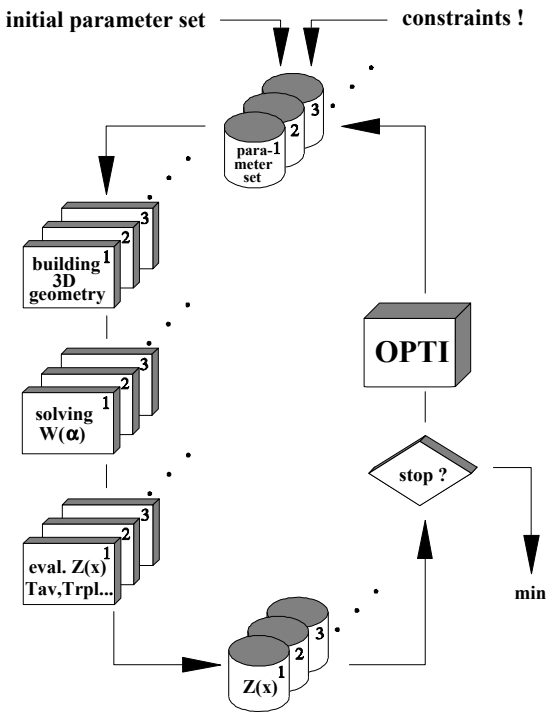

Fig. 1. Process control.

numerical optimisation takes the results from the field calculation and decides whether to stop the optimisation or to continue in generating a new set of objective variables. In this paper this is done with a stochastic search strategy, the evolution strategy.

2. Numerical Optimisation

Stochastic optimisation techniques such as evolution strategy and simulated annealing are attracting a great deal of interest due to their

- insensibility to disturbances,
- easy treatment of constraints,
- straight forward implementation,
- independence of derivatives,
- stable solutions.

Their main advantage is the insensibility to stochastic disturbance of the objective function caused by numerical evaluation. This insensibility results out of the non-deterministic search and the fact that no derivatives are needed. The second important property is the easy treatment of constraints. A complicated transformation into an unconstrained problem formulation is not necessary.

The generation of the different configurations is independent. This offers the opportunity to run the algorithm on parallel computers. Figure 1 illustrates this process reducing the high computational cost.

2.1 Evolution Strategy

In this paper only higher evolution strategies are taken into account. More detailed information can be found in [1,4].

Numerical optimisation requires a single function,

$$Z(\mathrm{x}) = Z(x_1, x_2, ..., x_n) \quad \rightarrow \quad \min. \tag{1}$$

to be minimised. This function is called the objective- or quality-function. It depends on all design parameters involved. By minimising with respect to more than one goal $Z_1, Z_2, \ldots, Z_n$ simultaneously, the single aim has to be weighted in a linear combination. With Z as the total quality and a_i the weighting factors it can be formulated as:

$$Z = \sum_{i=1}^{n} a_i \, Z_i \tag{2}$$

The evolution strategy copies the natural principles of mutation and selection (*survival of the fittest*) by the biological evolution into the technical optimisation problem.

The basic concept of the evolution strategy is founded in the substitution of DARWIN's notation of fitness to the quality of a technical product. The driving force in the optimisation process is the repetition of mutation and selection in successive steps. The mutation of the objective variables of an initial generation (parents) leads to a number of offspring's. The variables of one child may depend on multiple parent variable vectors. The best offspring's are selected to form the next generation.
In the optimisation process the repetition of mutation and selection of the objective variables leads from a temporary to an improved solution. With μ the number of parents, λ the number of offspring's or children and ρ a hereditary factor, at the $(\frac{\mu}{\rho}, \lambda)$-strategy ρ parent vectors contribute to the creation of a child. 1/ρ of the properties of one parent is transmitted to a child.

Mutation of an object is done with random additions to the object variables. For iteration step (k) the new variable $x_{C,i}^{(k)}$ is created from the parent variable $x_{P,i}^{(k)}$

$$x_{C,i}^{(k)} = x_{P,i}^{(k)} + \delta_{C,i}^{(k)} \; p_i^{(k)} \quad \text{with} \quad i = 1(1)n \tag{3}$$

To transmit the step width $\delta_{C,i}^{(k)}$ of the parent generation to the child generation, the step length of the randomly chosen parents is taken to build an average value.

$$\delta_{C,i}^{(k)} = \frac{1}{\rho} \sum_{j=1}^{\rho} \delta_{P,j}^{(k)} \left(z_j^{(k)}(\mu)\right) \quad \text{with} \quad \begin{cases} i = 1(1)n \\ j = 1(1)\rho \end{cases} \tag{4}$$

$z_j^{(k)}(\mu)$ is an uniformly distributed random integer number out of the interval $[1, \mu]$. To obtain the mutation step width the before mentioned average value is multiplied by a step width factor α.

$$\delta_{C,i}^{(k)} = \begin{cases} \delta_{C,i}^{(k)} \cdot \alpha & : i = 1(1)\lambda/2 \\ \delta_{C,i}^{(k)} \cdot 1/\alpha & : i = \lambda/2 + 1(1)\lambda \end{cases} \tag{5}$$

3. Numerical Field Computation

The method to compute the field of the electrostatic micromotors used is the 3d finite element method. Earlier work has been limitted to 2d finite elements [2]. For radial flux motors this is possible since their geometry does not vary in the axial direction, see fig. 2A, but due to that the axial lengt is short compared with the rotor radius 3d analysis is to prefer. For the axial flux motors, 3d analysis is required due to the geometry, see fig 2B.

3.1 Automated building of 3d meshes

Building 3d meshes is normally a time consuming process. Therefore performing optimisation in 3d is very tedious since a large number of models, slightly different from one another, must be built and analysed. For micromotor structures the required labour is even vaster since for every model the analysis normally must be carried out for a number of rotor positions, in order to obtain macroscopic parameters as torque and capacitance as function of the rotor position. For most 3d finite element packages a new rotor position requires a new mesh to be generated. In this paper the fast and reliable extrusion-based 3d mesh generator is automated in such a way that a large range of different motor geometries can be generated, with a fully arbitrarily choice of the rotor position.

3.2 Periodic geometry

All electric rotating motors inherently possess some kind of periodicity. Typically each motor has a stator and a rotor where the geometric period, in degrees, is defined as the pole pitch τ. Each periodic geometry also has an extension within the pole pitch. This extension is referred to as the polar arc τ'.

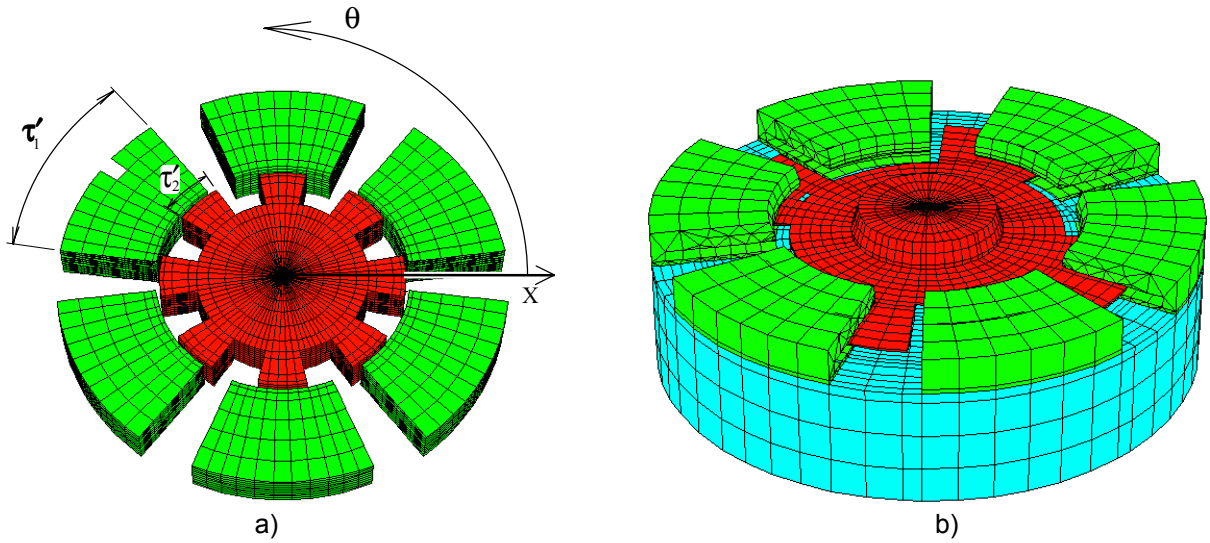

Fig. 2. a) 3d mesh of a 6/8 pole electrostatic radial flux micromotor and b) a 6/4 pole construction.

With these two parameters, the pole pitch τ and the polar arc τ', it becomes easy to describe where the sides of the stator teeth and rotor teeth, parallel with the rotor axis, are located in the motor. If the motor is scanned in the positive θ direction, see fig. 2, the following equations define the location of the front-sides and the back-sides of the stator teeth.

$$\begin{aligned} \Theta^{n}_{1,\text{front}} &= \left(\frac{\tau_1 - \tau'_1}{2}\right) + n \cdot \tau_1 \\ \Theta^{n}_{1,\text{back}} &= \left(\frac{\tau_1 + \tau'_1}{2}\right) + n \cdot \tau_1 \\ \text{where} \quad n &= 0(1)\left(\frac{360° - \tau_1}{\tau_1}\right) \end{aligned} \tag{6}$$

The reference point for θ is chosen in the middle between two stator teeth. By introducing the offset angle α accounting for the rotor position, the same may be done for the rotor.

$$\begin{aligned} \Theta^{n}_{2,\text{front}} &= \left(\frac{\tau_1 - \tau'_2}{2}\right) + n \cdot \tau_2 + \alpha_2 \\ \Theta^{n}_{2,\text{back}} &= \left(\frac{\tau_1 + \tau'_2}{2}\right) + n \cdot \tau_2 + \alpha_2 \\ \text{where} \quad n &= 0(1)\left(\frac{360° - \tau_2}{\tau_2}\right) \end{aligned} \tag{7}$$

The motor geometry can, in the general case, be split in more than 2 periodic geometries. Subscripts 1 and 2 indicate parameters for the stator and rotor respectively.

3.3 The extrusion techique

The 3d meshes are built using an extrusion technique. With this technique many 2d meshes, placed at different locations in space, are connected in order to generate the 3d mesh. The reference 2d mesh is referred to as the baseplane, see fig. 3. Each plane is applied with extrusion data describing its position in space. The extrusion technique, discussed in this paper, only uses rotation around the y-axis, thus θ, to define the extrusion data. One vertical side of the base-plane should coincide with the global y-axis. Since each copy of the base-plane only gets the θ parameter as extrusion data, one of the vertical sides of all planes also coincide, with the global y-axis, i.e. the centre of the rotor shaft, see fig. 4.

From the knowledge of the number of poles, the polar arc τ' of stator and rotor, and the rotor position, and using Eqns. (6) and (7) it is easy to find where planes must be located. For each of the periodic geometries 4 different type of actions (sequence of relabeling and/or constraining) are defined. Types 1 and 2 define a front and a backside respectively, on e.g. a rotor tooth. Types 3 and 4 define a plane inside or outside of e.g. a rotor tooth. These four actions define every plane for each periodic geometry. Thus the maximum number of different plane-types required to construct a model is 4^N, where N is the number of periodic geometries in the model. These planes are generated in advance and are sufficient to define all possible combinations of τ, τ' and α. This means that ones the planes are generated the remaining task is to find out at what angle which kind of plane must be located. This is performed with repetitive use of Eqns. (6) and (7) and a sorting algorithm. This sorting algorithm finds what the next plane must be from knowing the previous. A front-plane must be followed by and inside-plane, an inside-plane by a back-plane and so on. The angle between two consecutive planes has to be chosen depending on the size of the elements in the base-plane and the required aspect ratio of the 3d elements, the tetrahedrons. This implies that the same kind of planes sometimes has to be repeated with the desired angle between them in order to improve the aspect ratio of the tetrahedrons. This is automatically controlled.

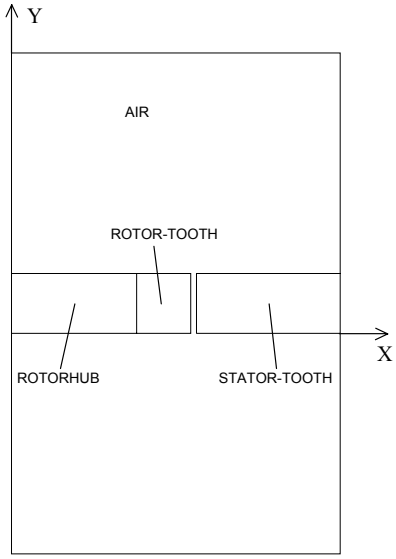

Fig. 3. Base-plane used when generating model of figure 2.

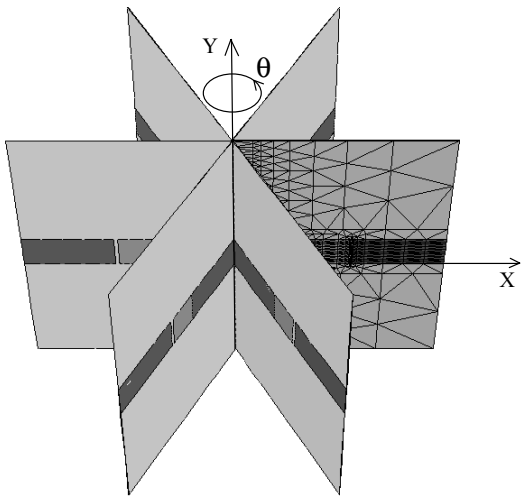

Fig. 4 Copies of the base-plane mesh, placed at different angles θ.

3.4 Performance

The major advantage of automating the extrusion-based mesh generator, rather then a solid modelling mesh generator, is speed. To generate a motor model with approximately 100'000 tetrahedrons takes, from the instant that the parameters are entered to the model is built ready for the solver, less than 10 minutes on a HP715. Once the different kinds of planes are generated, it takes always less then 5 min. This should be compared with typically more than 45 min for a solid modelling mesh generator.

4. Equivalent Circuit Model

The application of the methods mentioned is demonstrated by optimising two electrostatic micromotors. The objective is to maximise the average torque. The average torque is calculated for the best possible excitation of each motor. To find this excitation an equivalent circuit technique has been used. Although the finite element calculation together with discrete fourier transform, DFT, can provide $W_e(\alpha)$, stored electric energy as function of the rotor position, in the form of a fourier series, is it only valid for that or those excitations applied during the finite element calculations.

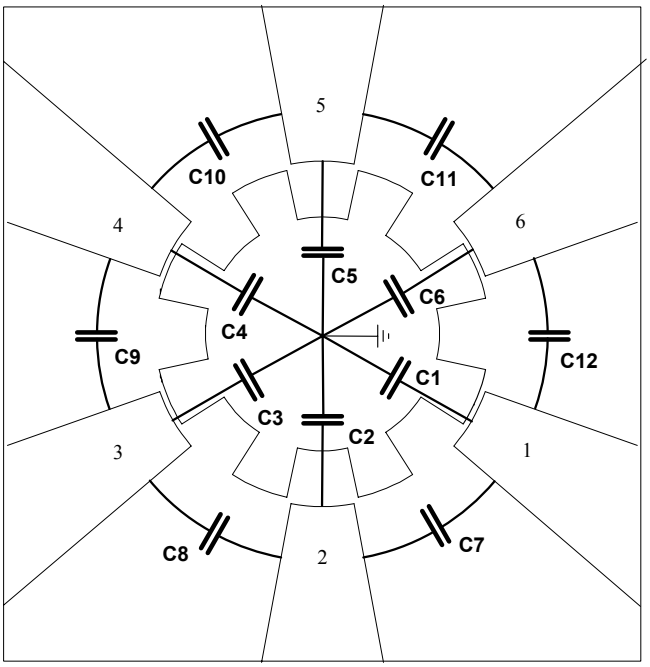

Fig. 5. Equivalent circuit for an electrostatic motor with 6 stator poles.

The information gained from two different excitations over the rotor positions is however sufficient to create an equivalent circuit describing the motor geometry. The equivalent circuit used for a 6/8 pole motor is shown in figure 5 and consists of 12 capacitors, two times the number of stator electrodes (poles). Their capacitance varies with the rotor position α. There are only two principally different capacitances. Writing $C_{SR}^{k}(\alpha)$ for the capacitance between stator electrode *k* and the rotor, C1 to C6, and $C_{SS}^{k}(\alpha)$ for the capacitance between stator electrode *k* and the next stator electrode, C7 to C12, it can readily be seen that he difference between capacitances with different index *k* is only a phase shift equal to a multiple of the stator pole pitch τ_2. With two different excitations for n rotor positions, the stored energy is calculated and the system of equations,

$$\begin{aligned} W_e(\alpha_1) &= \tfrac{1}{2}\left[\sum_{k=1}^{n_p} C_{SR}^{k}(\alpha_1)\cdot V_k^2 + \sum_{k=1}^{n_p} C_{SS}^{k}(\alpha_1)\cdot (V_{k+1}-V_k)^2\right] \\ &\vdots \\ W_e(\alpha_n) &= \tfrac{1}{2}\left[\sum_{k=1}^{n_p} C_{SR}^{k}(\alpha_n)\cdot V_k^2 + \sum_{k=1}^{n_p} C_{SS}^{k}(\alpha_n)\cdot (V_{k+1}-V_k)^2\right] \end{aligned} \qquad (8)$$

$$\text{where} \quad V_{n_p+1} = V_1$$

can be solved. Once $C_{SR}^{k}(\alpha)$ and $C_{SS}^{k}(\alpha)$ are found the torque is calculated using analytic differentiation.

$$T(\alpha) = \frac{\partial W_e(\alpha)}{\partial \alpha} \tag{9}$$

4.1 Optimum excitation sequence

Having the equivalent circuit any kind of excitation wave form can easily be applied. The block-wave is applied throughout the optimisation, since it is the most powerful one. To avoid or at least minimise radial forces on the rotor shaft, the motors have to be excited symmetrically. Figure 6 shows the possible symmetric excitations of a motor with 6 stator electrodes, where the grey electrodes are excited to 1 V and the rotor and the white electrodes are kept at 0 V. By applying these excitations to the equivalent circuit the torque characteristics over the rotor positions can be calculated. Figure 7 shows the torque produced over one electric period for the six different excitations from figure 6.

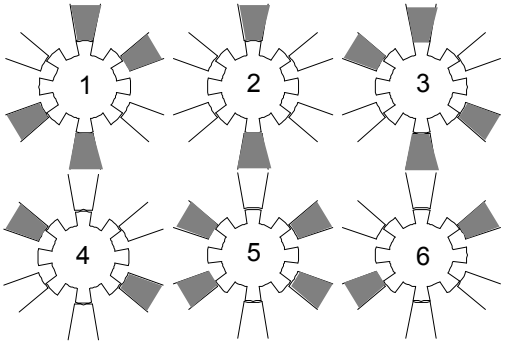

Fig. 6. Possible symmetric excitations of a motor with six electrodes.

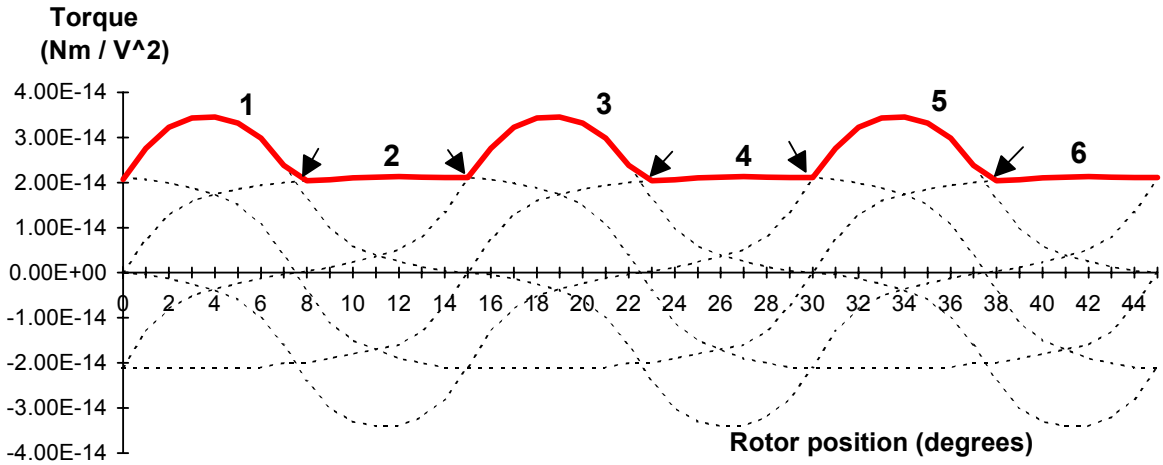

Fig. 7. Produced static torque over one electric period for 6 different excitations on a 6/8 pole motor.

By switching from one excitation to another, at the crossovers marked by arrows, the optimum excitation sequence is achieved. The average torque T_{av} is then calculated by integration of the curve always following the highest torque. The torque ripple T_{rpl} is

$$T_{rpl} = \frac{T_{max} - T_{min}}{T_{av}} \tag{10}$$

5. Optimisation of a Micromotor

The geometry of the micro motors from fig. 2 is modelled by 2 design variables. The free parameters are the pole arcs of the rotor and stator teeth. Due to constraints resulting from the fabrication conditions the other design variable were set to fixed values. For the motor from fig. 2a the air gap is fixed to a value of 10 µm, the rotor height to 100 µm and the outer diameter of the rotor is 600 µm. For the motor from fig. 2b the air gap is fixed to a value of 3 µm, the rotor thickness to 4 µm and the outer diameter of the rotor is 320 µm.

6. Results

Figure 8 shows a surface fit through the selections when the objective was to maximise the average torque. Figure 9 shows a surface fit of the torque ripple for the same selections of design parameters. Both figures refers to optimisation of the 6/8 pole motor with radial flux, see fig. 2a. The maximum average toque for this motor is calculated to be 0,1 nNm for an excitation of 50 V.

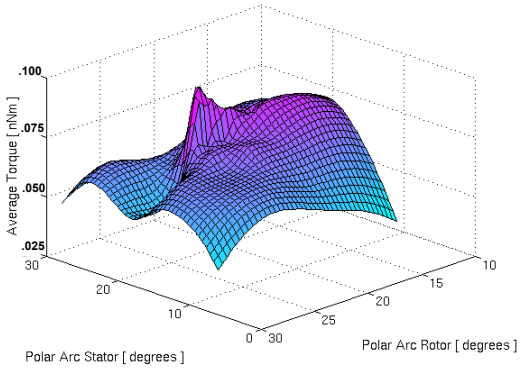

Fig. 8. Average torque as function of combinations of polar arcs in the stator and the rotor, represented by a surface fit of the selections during the optimisation

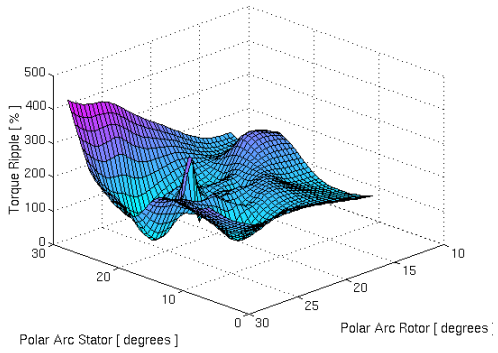

Fig. 9. Torque ripple as function of combinations of polar arcs in the stator and the rotor, represented by a surface fit of the selections during the optimisation.

Figure 10 and 11 shows for the 6/4 pole axial flux motor from fig.2b the same properies as fig. 8 and 9 does for the radial flux motor. The surface fits in fig. 10 and 11 are however from 18 selections of design parameters made according to the optimisation strategy called *surface responce methodology*. With this technique first 9 selections of design parameters was made. A funtion is fitted to the resulting 9 torques and in the area of max torque a new set of 9 selections is made. A new funtion is fitted to all 18 torques. The maximum average torque of the axial flux motor from fig.2b was calculated to be 0,15 nNm for an excitating of 50 V.

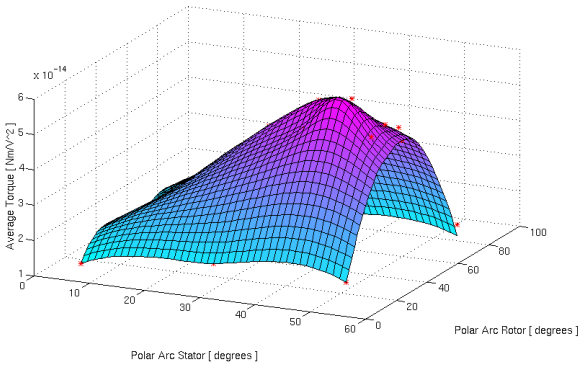

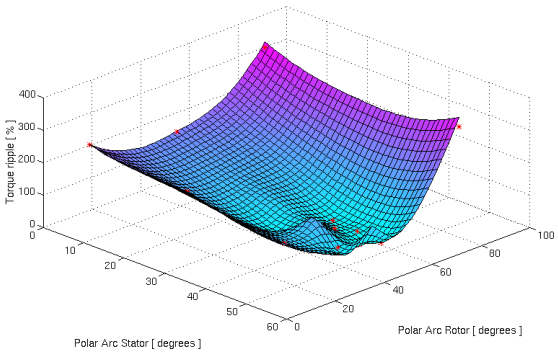

Fig. 10. Average torque of axial flux motor.

Fig. 11. Torque ripple of the axial flux motor.

It can be seen from figure 8 and 10 that the average torque has one global maximum for two design variables, and the torque ripple one local minimum for almost the same combination of parameters.

This was found also from the 2d optimisations [2]. The shape of the surface fit for the radial flux motor, fig. 8 and 9, is however by far not so smooth as it is in the 2d study. This is most probably due to the reduced number of rotor positions used in the 3d case in combination with the use of Fourier series to

fit eqn. (8). In the 2d study and in the 3d study, one electric period was discretised with 45 and 18 rotor positions respectively. The torque is calculated using the derivative of eqn. (8) and the discrete fourie transform (DFT) this shows extra oscillations when eqn. (8) tend to be flat and approximated with to few points. The reason why the number of rotor positions was reduced is the computation time. The computational cost for one rotor position is in the range of 20 min for a first order solution and 45 min for a second order solution.

The axial flux motor has shown to be less sensitive to the use of DFT. The stored energy as function of the rotor position can be fitted with only a few number of harmonics.

7. Conclusion

An application of the evolution strategy, a method for minimisation of functions of continuous variables is presented. Numerical field computation to evaluate the objective function is performed using a three dimensional finite element method.

Clearly the presented technique for automating the model generation and extracting global quantities as average torque offers a tool well worth exploring further. However, another curve fitting function, which should serve to improve the differentiation of the stored energy expressed by equivalent capacitors eqn. (8) must be chosen. This will be done in order to improve the accuracy of especially the torque-ripple. A possible choice is to use the cubic spline interpolation.

The optimisation method decribed in the paper is very easy to implement since it need no other knowlege of the system than constraints. It does however need many function evaluations to find the global optimum. Since for 3d finite elements, the evaluation is rather timeconsuming there is a risk that many hours are lost before it can be stated that the accuracy of the function evaluations are poor for some of the selections but not for all. This was the case for the optimisation of the radial flux motor. It is of great importance that the quality evaluation works well in the whole range of design variables.

The generation of the different configurations is independent. This offers the opportunity to run the algorithm on parallel computers reducing the high computational cost.

References

[1] K. Hameyer and R. Hanitsch: "Numerical optimization of the electromagnetic field by stochastic search and MEC-model", *Proc. Conf. COMPUMAG*, November 1993, Miami, USA.

[2] T.B. Johansson, M.Van Dessel, R.Belmans, W.Geysen, R.Hanitsch: "An optimisation scheme of electrostatic micromotors based on an Equivalent Circuit - Finite Element approach.", *Proc. Conf. ICEM 1992*, UMIST Manchester, UK, pp. 1157-1161.

[3] W. Trimmer "Microrobots and Micro-mechanical systems", Sensors and Actuators Vol. 19, 1989, pp 267-287.

[4] H.-P., Schwefel: "Numerical optimization of computer models", *Wiley & Sons*, Chichester, 1981.